Sensor and Simulation Notes
Note 561
26 December 2012

A Method for the Analysis and Design of Coaxial Switched Oscillators Using Chain Parameters

Felix Vega
EMC Laboratory, Swiss Federal Institute of Technology of Lausanne (EPFL), Switzerland
Electrical and Electronic Engineering Department, National University of Colombia, Bogota
felix.vega@epfl.ch

Farhad Rachidi
EMC Laboratory, Swiss Federal Institute of Technology of Lausanne (EPFL), Switzerland

Nicolas Mora
EMC Laboratory, Swiss Federal Institute of Technology of Lausanne (EPFL), Switzerland

Bertrand Daout
Montena Technology, Rossens, Switzerland

Nestor Peña
Electrical and Electronic Engineering Department, Los Andes University, Bogota, Colombia

Francisco Roman
Electrical and Electronic Engineering Department, National University of Colombia, Bogota

Abstract –

We investigate in this paper the behavior of a switched oscillator (SWO) by considering the frequency-dependency of the input impedance of the antenna. The analysis is performed using the chain-parameter (ABCD) representation of the system, which allows obtaining a semi-analytical solution suitable for the design and optimization of the SWO. The proposed approach was applied to the analysis of a SWO connected to a monopole antenna for which the transfer function, and the radiated field, in frequency- and time-domain are evaluated.

1. INTRODUCTION

Switched Oscillators (SWOs) are quarter wave oscillators that were proposed by Baum in [1] for the generation of mesoband high power electromagnetic fields. SWOs have been studied during the past years, and they have shown promising results in the generation of high power electromagnetic oscillatory signals in the range of hundreds of MHz to a few GHz [2]-[3].

In [2], Giri *et al.* described a set of coaxial SWOs connected to helical antennas. In their analysis, the oscillator was represented using cascaded uniform transmission lines and its response was obtained by simulations using traditional circuit codes. The model yielded accurate results in predicting the central frequency and the quality factor Q of the SWOs. In [2], the helical antenna was represented by a constant, real impedance. [3]. A similar assumption was also made by Armanious *et al.* in [3], when considering the connection of a monocone antenna to an SWO. It is important to realize that this assumption is only valid for a set of frequencies in which the input impedance of broadband antennas such as helices and monocones exhibit a low reactance and an almost constant resistance. However, if a narrow band antenna is connected to an SWO, the accurate simulation of the system requires taking into account the frequency dependence of the input impedance of the antenna. Note that the work of Armanious et al. [3] was based on a full wave analysis in which the frequency dependence of the antenna can in principle be taken into account.

Consider the geometry of the SWO proposed in [2], but connected to a monopole antenna as schematically illustrated in Figure 1. Notice that the electrodes forming the spark gap configure a radial transmission (RTL) that progressively becomes a low-impedance coaxial transmission line. At the end of the coaxial transmission line, an antenna (in this case a monopole) is connected through a DC blocking capacitor.

In this work, a detailed frequency domain analysis of the SWO presented is made by using the so-called chain parameters. Such methodology enables the possibility of estimating the output voltage of the oscillator as the product of the chain parameters of each separate section composing the structure. The effect on the output frequency spectrum due to the insertion of each of the sections of the SWO (namely the spark gap, the RTL, the coaxial TL, the blocking capacitor and the antenna) can be evaluated in a straightforward way. Moreover, the ABCD matrix representation permits to obtain a semi-analytical solution of the radiated field, suitable for the design and optimization of the SWO.

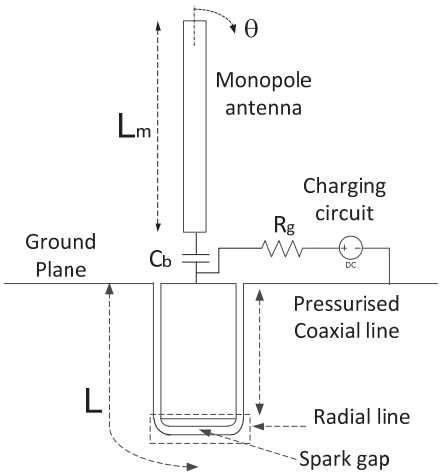

Figure 1 A monopole antenna integrated into a SWO

The choice of the monopole antenna was made to illustrate the procedure with a highly resonant structure for which the input impedance can be easily calculated with classical EM codes. Otherwise, the proposed methodology is applicable to any kind of antenna.

A preliminary analysis has been presented by the authors in [4]. In the present paper, we present a more detailed analysis of the ABCD parameters of each section of the SWO, we explain the influence of the spark impedance on the transfer function of the SWO, and we derive a transfer function for the electric field radiated by the antenna.

2. CIRCUIT REPRESENTATION OF THE SWO

The SWO can be represented by using the equivalent circuit shown in Figure 2. The model consists of a voltage source, a radial transmission line (RTL), a main coaxial transmission line, a matching transmission line section, a DC-blocking capacitor, and finally the antenna.

We propose to analyze this system using two-port networks [5] and in particular using the so-called chain matrix parameters (also known as the ABCD or transmission matrix).

Each section of the SWO is represented as a two-port network characterized by its chain parameters. The total transfer function between the excitation voltage at the spark gap and the input voltage at the antenna, as a function of frequency, can be calculated by multiplying the chain parameter matrices associated with each section. The time domain voltage at the input of the antenna can then be obtained by an inverse Fourier transformation.

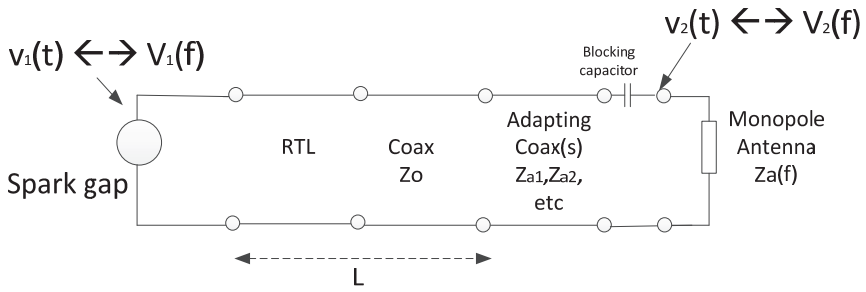

Figure 2 Transmission line system representing the SWO

We applied this method to the analysis of one of the SWOs presented by Giri *et al*. in [2], which is composed of a radial transmission line, a main coaxial line of length L_{coax}=25.8 cm and a characteristic impedance Z_{coax}=3.7 Ω, two adapting transmission lines of impedances Z_{adapt1}=23 Ω and Z_{adapt2}=66 Ω, a DC-blocking capacitor C_b=20 pF, and a helical antenna. The SWO is resonant at a frequency of 200 MHz. To illustrate the advantages of the presented methodology, instead of considering a helical antenna (which is characterized by a low reactance over a significant bandwidth [2]), we used a monopole antenna since it exhibits a more pronounced frequency dependence. For the sake of simplicity, we neglected the matching transmission lines proposed in the original design.

3. RADIAL TRANSMISSION LINE

The geometry of the electrodes in the spark gap region can be represented as a radial transmission line (RTL). The RTL is a non-uniform transmission line that exhibits a high characteristic impedance at the discharge point. As the wave propagates from the switch region toward the coaxial line, the characteristic impedance drops rapidly and tends to the value of Z_{coax}.

The RTL can be decomposed into a series of cascaded uniform transmission lines, as suggested in [2] and illustrated in Figure 3. It consists of 20 segments, each one having a average length ΔL = 1 mm. We can assume that the characteristic impedance of the n-th segment can be calculated using:

$$Z_{RTL,n}(f) = \frac{60 d_n}{r_n} \tag{1}$$

where d_n is the distance between the inner and outer conductors, measured at the center of the segment, and r_n is the distance between the midpoint of the segment and the symmetry axis, as shown in Figure 3.

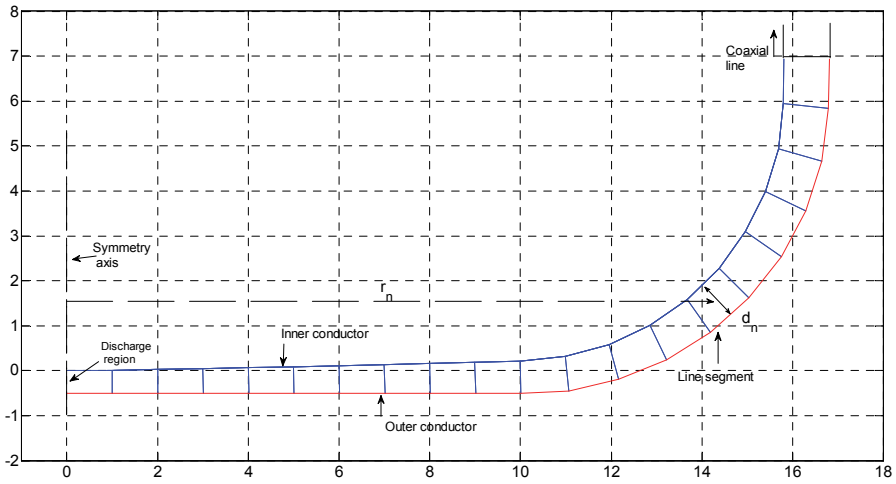

Figure 3 Discretization of the Radial Transmission line

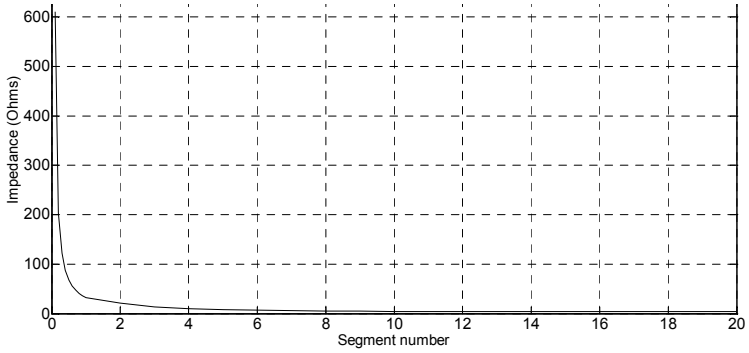

Figure 4 Characteristic impedance variation along the RTL

Figure 4 shows the variation of the characteristic impedance of the RTL from its axis up to reaching the coaxial transmission line. The impedance function varies from infinite, at the axis of symmetry, up to join the impedance of the coax. This convergence can be explained as follows:

At the point of connection between the coax and the RTL:

$$d_m = r_0 - r_i$$
$$r_m = \frac{r_0 + r_i}{2} \tag{2}$$

The impedance of the last segment (*m-th* term) of RTL is therefore:

$$Z_{RTL,m}(f) = 120\left(\frac{r_0 - r_i}{r_0 + r_i}\right) \tag{3}$$

On the other hand, the impedance of the coaxial transmission line is:

$$Z_{Coax} = 60Ln\left(\frac{r_o}{r_i}\right) \tag{4}$$

The logarithmic term in Equation (4) can be expanded as a Maclaurin series [6]:

$$Z_{coax} = 60Ln\left(\frac{r_o}{r_i}\right) = 60\left(2\left[\left(\frac{\frac{r_o}{r_i}-1}{\frac{r_o}{r_i}+1}\right)+\frac{1}{3}\left(\frac{\frac{r_o}{r_i}-1}{\frac{r_o}{r_i}+1}\right)^3+\frac{1}{5}\left(\frac{\frac{r_o}{r_i}-1}{\frac{r_o}{r_i}+1}\right)^5+\ldots\right]\right) \tag{5}$$

If $r_o \approx r_i$, Equation (5) can be approximated as:

$$Z_{coax} = \frac{60}{\sqrt{\varepsilon_r}}Ln\left(\frac{r_o}{r_i}\right) \approx 120\left(\frac{r_o - r_i}{r_o + r_i}\right) = Z_{RTL,m}(f) \tag{6}$$

This means that the assumption on the model of the radial transmission line impedance is valid only if the condition $r_o \approx r_i$ is respected (low impedance coax). Otherwise the bend in the RTL is too significant to be neglected and a different impedance model should be adopted.

3.1 Chain (ABCD) matrix representation of the SWO

In the original work of Giri *et al*. [2], a circuit simulation code was used to represent each transmission line segment. In this work we use the chain-parameter (ABCD matrix) representation of the system that will permit to obtain a semi-analytical solution suitable for the design and optimization of the SWO.

The ABCD parameters of a two-port network can be defined using the diagram presented in Figure 5 [5]:

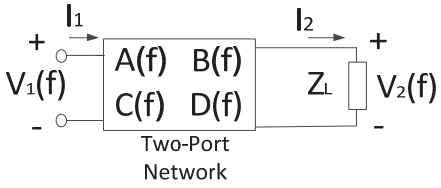

Figure 5 ABCD representation of a two-port network

The input and output parameters of the network are related by the equation:

$$\begin{bmatrix} V_1(f) \\ I_1(f) \end{bmatrix} = \begin{bmatrix} A(f) & B(f) \\ C(f) & D(f) \end{bmatrix} \begin{bmatrix} V_2(f) \\ I_2(f) \end{bmatrix} \tag{7}$$

From which the voltage transfer function can be obtained as:

$$V_2(f) = \frac{Z_L(f)V_1(f)}{Z_L(f)A(f) + B(f)} \tag{8}$$

The main advantage of using the ABCD representation is that the resulting ABCD matrix of several networks connected in cascade can be obtained by multiplying the ABCD matrices of the individual systems.

The segments of the RTL can be represented using this formulation. The ABCD matrix of the *n*-th segment of the RTL is given by [5]:

$$\begin{bmatrix} A_n(f) & B_n(f) \\ C_n(f) & D_n(f) \end{bmatrix} = \begin{bmatrix} \cosh(j\beta\Delta L) & Z_{0n}(f)\sinh(j\beta\Delta L) \\ \dfrac{\sinh(j\beta\Delta L)}{Z_{0n}(f)} & \cosh(j\beta\Delta L) \end{bmatrix} \tag{9}$$

where Z_{0n} is the characteristic impedance of the segment, $\beta=2\pi/f$, f is the frequency and ΔL is the length of the segment.

The ABCD parameters of the coaxial transmission line are:

$$\begin{bmatrix} A_{Coax}(f) & B_{Coax}(f) \\ C_{Coax}(f) & D_{Coax}(f) \end{bmatrix} = \begin{bmatrix} \cosh(j\beta L_{Coax}) & Z_{Coax}\sinh(j\beta L_{Coax}) \\ \dfrac{\sinh(j\beta L_{Coax})}{Z_{Coax}} & \cosh(j\beta L_{Coax}) \end{bmatrix} \tag{10}$$

The whole system (RTL + coaxial segment + antenna) can be represented by the cascade of all the two-port networks; each one characterized by its ABCD matrix (see Figure 6).

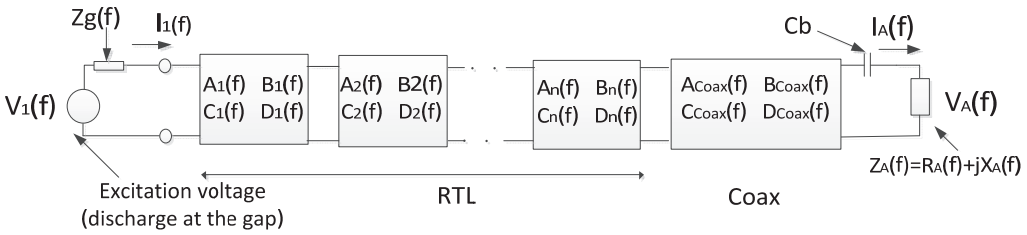

Figure 6 Representation of the SWO using the cascade of all the two-port networks characterized by their ABCD matrices.

In the diagram of Figure 6, V_1 is the voltage produced by the spark gap, Z_g is the spark gap impedance, V_A is the input voltage on the antenna terminals, C_b is a blocking capacitor, Z_A is the input impedance of the antenna, R_A is the radiation resistance of the antenna, X_A is the reactance of the antenna.

The chain parameter matrix of the whole system can be expressed as:

$$\begin{bmatrix} A_{Total}(f) & B_{Total}(f) \\ C_{Total}(f) & D_{Total}(f) \end{bmatrix} = \begin{bmatrix} 1 & Z_g(f) \\ 0 & 1 \end{bmatrix} \times \prod_{n=1}^{20} \begin{bmatrix} A_n(f) & B_n(f) \\ C_n(f) & D_n(f) \end{bmatrix} \times \begin{bmatrix} A_{Coax}(f) & B_{Coax}(f) \\ C_{Coax}(f) & D_{Coax}(f) \end{bmatrix} \times \begin{bmatrix} 1 & \frac{1}{j2\pi fC_b} \\ 0 & 1 \end{bmatrix} \tag{11}$$

Where:

$Z_g=R_g+jX_g$ is the impedance of the spark gap[1].

and the matrix Π operator is defined as [7]:

$$\prod_{n=1}^{m}\begin{bmatrix} A_n(f) & B_n(f) \\ C_n(f) & D_n(f) \end{bmatrix}=\begin{bmatrix} A_1(f) & B_1(f) \\ C_1(f) & D_1(f) \end{bmatrix}\times\begin{bmatrix} A_2(f) & B_2(f) \\ C_2(f) & D_2(f) \end{bmatrix}\times\ldots\times\begin{bmatrix} A_m(f) & B_m(f) \\ C_m(f) & D_m(f) \end{bmatrix}$$

The relationship between the input and output voltages and currents can be therefore calculated using:

$$\begin{bmatrix} V_1(f) \\ I_1(f) \end{bmatrix}=\begin{bmatrix} A_{Total}(f) & B_{Total}(f) \\ C_{Total}(f) & D_{Total}(f) \end{bmatrix}\begin{bmatrix} V_A(f) \\ I_A(f) \end{bmatrix}=\begin{bmatrix} A_{Total}(f) & B_{Total}(f) \\ C_{Total}(f) & D_{Total}(f) \end{bmatrix}\begin{bmatrix} V_A(f) \\ \frac{V_A(f)}{Z_A(f)} \end{bmatrix} \quad (12)$$

from which the voltage on the antenna can be determined using equation (8):

$$V_A(f)=\frac{Z_A(f)V_1(f)}{Z_A(f)A_{Total}(f)+B_{Total}(f)} \quad (13)$$

The impedance of the antenna (Z_A) is a complex number, formed by a resistive ($R_A(f)$) and a reactive term ($X_A(f)$), $Z_A=R_A(f)+jX_A(f)$.

A transfer function $T(f)$ relating the voltage at the input of the antenna and the excitation voltage can be defined as:

$$T(f)=\frac{V_A(f)}{V_1(f)}=\frac{Z_A(f)}{Z_A(f)A_{Total}(f)+B_{Total}(f)} \quad (14)$$

4. SOURCE REPRESENTATION

The integration of a full electro-dynamic model of the spark into the ABCD equivalent model requires taking into account the time-dependent spark gap resistance and inductance, which is a non-trivial task (see e.g.[8]). In this study, we used a simplified source model that includes the slow charging phase of the SWO, followed by a fast drop of the voltage at the spark gap. The arc resistance and inductance are considered constant and their values are determined using the static values proposed by Martin [9].

A rectangular voltage pulse with a long risetime (~400 ns) simulating the charging phase of the SWO, followed by a fast decay time ((~100 ps) was selected for V_1. The voltage source is connected in series to a constant resistance R_g and a constant inductance L_g that slows down

[1] It is worth noting that nonlinear effects were disregarded in the analysis.

the falling edge of V_1 to the order of magnitude reported in the literature [9]. As a result, a maximum charging voltage of 40 kV and values of R_g=0.1 Ω and L_g= 0.25 nH were adopted.

Figure 7 shows the excitation voltage ($V_1(f)$) in frequency and time domain ($v_1(t)$). The waveform was generated by using a modified version of the function presented by Giri in [10]:

$$V_1(f) = \left[\frac{V_o t_d}{(\beta + j2\pi f t_d)} e^{\frac{(\beta + j2\pi f t_d)^2}{4\pi}} \right]^* e^{-j2\pi t_s} \tag{15}$$

where β = 60e-3, t_d=0.1 ns, V_o= 40 kV, t_s=2000 ns, and * is the conjugate operator.

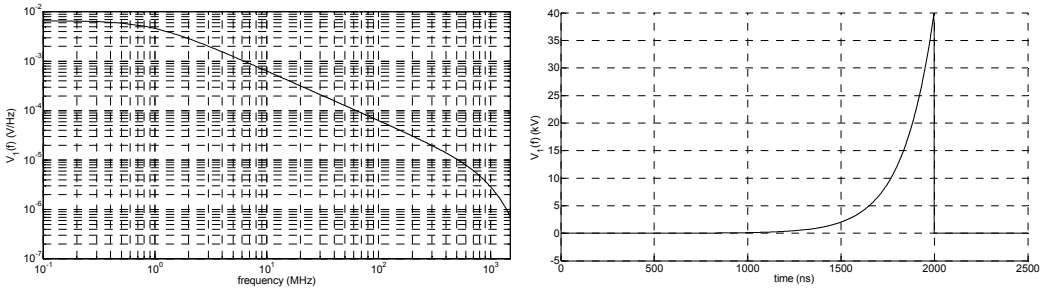

Figure 7 Excitation voltage in frequency domain (left) and time domain (right)

5. THE ABCD MATRIX AND RESONANCE FREQUENCY OF THE SWO

The resonance frequencies of the two-port network presented in Figure 6, are the frequencies in which the A and B terms of its ABCD matrix goes to zero [7]. This can be seen from Equation (14), according to which the voltage transfer function maximizes at the frequencies f_A, f_B where $A(f_A)$=0, $B(f_B)$=0:

$$\begin{aligned} T(f_B) &= \frac{V_A(f_B)}{V_1(f_B)} = \frac{1}{A(f_B)}; \quad B(f_B) = 0 \\ T(f_A) &= \frac{V_A(f_A)}{V_1(f_A)} = \frac{Z_A(f_A)}{B(f_A)}; \quad A(f_A) = 0 \end{aligned} \tag{16}$$

Given the fact that generally $|Z_A| > 1$, it can be concluded from (16) that it is desirable to work at the resonance frequency $f = f_A$ since it gives higher amplitude at the output, if the following condition holds:

$$|A(f_B)| > |B(f_A)| \rightarrow |T_A| > |T_B|$$

In what follows, we will be present the A and B chain parameters after progressively multiplying each section of the SWO, as schematically shown in Figure 6.

The magnitude of the A and B parameters of the RTL section are plotted in Figure 8. The ABCD matrix for the RTL is defined as:

$$ABCD_{RTL}(f)=\prod_{n=1}^{20}\begin{bmatrix} A_n(f) & B_n(f) \\ C_n(f) & D_n(f) \end{bmatrix} \tag{17}$$

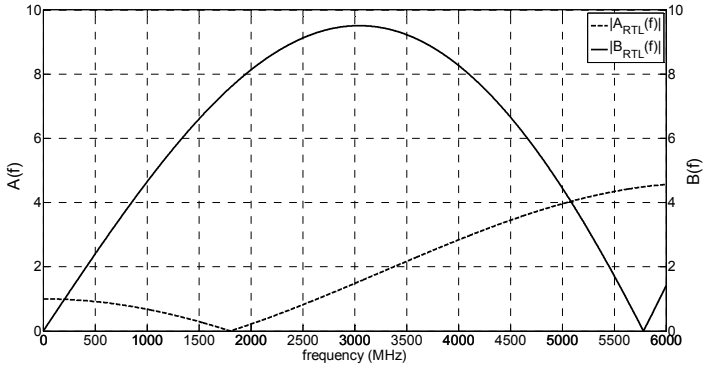

Figure 8 Parameters A and B of the RTL as a function of frequency

From (16) it follows that the higher resonance frequencies achievable with this RTL are located at $f_A=1.8$ GHz and $f_B=5.7$ GHz. These frequencies will be of course shifted after including the other sections of the SWO; especially the coaxial segment. The latter can be seen in Figure 9 where the magnitude of the A and B parameters of the product between the RTL and the coaxial section are plotted. This product can be expressed as:

$$ABCD_{RTL+Coax}=\prod_{n=1}^{20}\begin{bmatrix} A_n(f) & B_n(f) \\ C_n(f) & D_n(f) \end{bmatrix}\times\begin{bmatrix} A_{Coax}(f) & B_{Coax}(f) \\ C_{Coax}(f) & D_{Coax}(f) \end{bmatrix} \tag{18}$$

It can be seen in the plots of Figure 9 that after the coaxial section is added, the structure exhibits six resonance frequencies in the considered bandwidth, three due to the A term of the matrix and the other two due to the B term. The new resonance frequencies appear at f_{A1}=214 MHz (which is quite close to the intended resonance frequency), f_{B1}=432 MHz, f_{A2}=655 MHz, and f_{B2}=880 MHz. Notice that the frequencies where $|A(f)|$ maximizes correspond to the ones where $|B(f)|$ minimizes and vice versa.

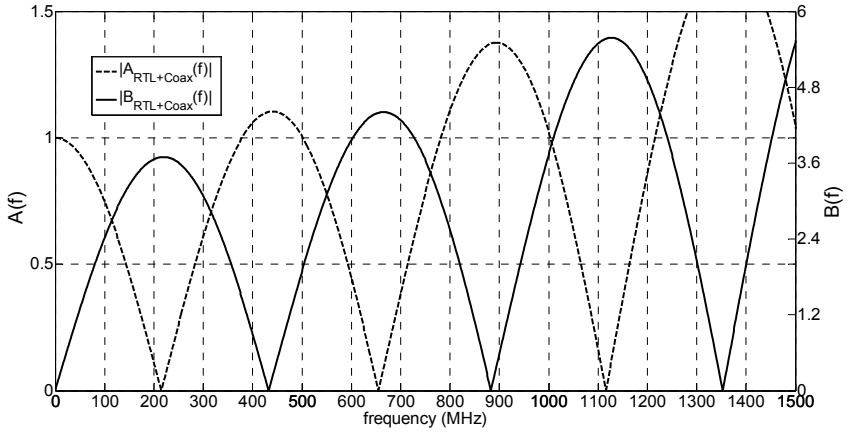

Figure 9 Parameters A and B of the RTL and the coaxial line

The effect of the spark gap impedance can be considered by including its ABCD matrix on the chain:

$$ABCD_{G+RTL+C} = \begin{bmatrix} 1 & Z_g \\ 0 & 1 \end{bmatrix} \times \prod_{n=1}^{20} \begin{bmatrix} A_n & B_n \\ C_n & D_n \end{bmatrix} \times \begin{bmatrix} A_{Coax} & B_{Coax} \\ C_{Coax} & D_{Coax} \end{bmatrix} \tag{19}$$

where $Z_g = R_g + j\omega L_g$, R_g=0.1 Ω, and L_g= 0.25 nH

The updated values of the magnitudes of A and B are plotted in Figure 10. As it can be seen from Figure 10, *A(f)* and *B(f)* are greater than zero at the resonance frequencies. This changes the maximum achievable values of the voltage transfer function in (13). A non-zero gap resistance (R_g) lowers the maximum amplitude of the transfer function, as the reflection of the wave at the spark gap is not total. This can be seen if the matrices product in (19) is further developed:

$$\begin{aligned} ABCD_{G+RTL+C} &= \begin{bmatrix} 1 & Z_g \\ 0 & 1 \end{bmatrix} \times \begin{bmatrix} A_{RTL+Coax} & B_{RTL+Coax} \\ C_{RTL+Coax} & D_{RTL+Coax} \end{bmatrix} \\ &= \begin{bmatrix} A_{RTL+Coax} + \left(R_g + jX_g\right) C_{RTL+Coax} & B_{RTL+Coax} + \left(R_g + jX_g\right) D_{RTL+Coax} \\ C_{RTL+Coax} & D_{RTL+Coax} \end{bmatrix} \end{aligned} \tag{20}$$

If the segments of the RTL and the coaxial section are considered as lossless, the terms $A_{RTL+Coax}$, and $D_{RTL+Coax}$ are real, and the terms $B_{RTL+Coax}$, and $C_{RTL+Coax}$ are imaginary. When the ABCD matrix of the spark gap is introduced, the terms $A_{G+RTL+C}$ and $B_{G+RTL+C}$ become complex:

$$
\begin{aligned}
\mathrm{Re}[A_{G+RTL+C}] &= A_{RTL+Coax} - X_g\ \mathrm{Im}[C_{RTL+Coax}] \\
\mathrm{Im}[A_{G+RTL+C}] &= R_g\ \mathrm{Im}[C_{RTL+Coax}] \\
\mathrm{Re}[B_{G+RTL+C}] &= R_g D_{RTL+Coax} \\
\mathrm{Im}[B_{G+RTL+C}] &= \mathrm{Im}[B_{RTL+Coax}] + X_g D_{RTL+Coax}
\end{aligned}
\tag{21}
$$

In principle, the real and imaginary parts of $A_{G+RTL+C}$ and $B_{G+RTL+C}$ should not be equal to zero at the same frequency, therefore the amplitudes of $A_{G+RTL+C}$ and $B_{G+RTL+C}$ will be greater than zero for all frequencies. The new imaginary and real parts of A and B appear because R_g is different from zero. We could reduce the value of R_g and discard these extra terms if we use a switch with a smaller d_{gap} (at a high pressure), however this solution is difficult to implement in most of practical applications.

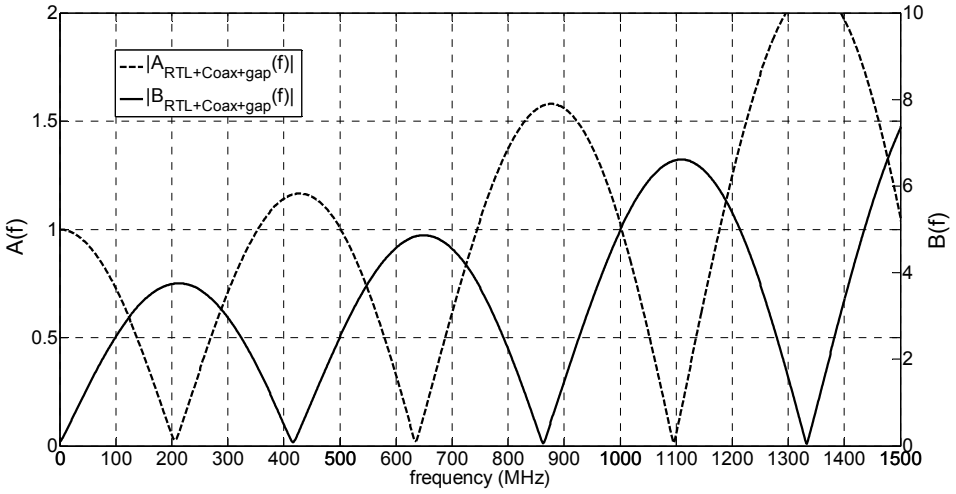

Figure 10 A and B parameters of the RTL and coaxial line, including the effect of the gap impedance

Finally, the *A* and *B* parameters of the whole system, including the blocking capacitor, are shown in Figure 11. Notice that the behavior of $A_{Total}(f)$ remains practically unchanged, with f_{1A}= 201 MHz and f_{2A} = 623 MHz. On the other hand, $B_{Total}(f)$ tends to infinity at $f=0$ due to the low-pass filtering function of the capacitor. The first zero of $B_{Total}(f)$ appears at about 190 MHz. Notice also that only the odd harmonics of 200 MHz have remained (compare Fig. 10 with Fig. 9).

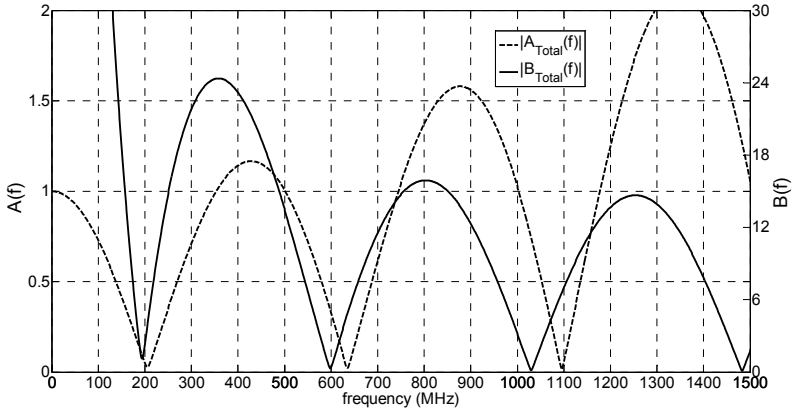

Figure 11 $A_{Total}(f)$ and $B_{Total}(f)$ parameters of the whole system.

6. APPLICATION: SWO CONNECTED TO A MONOPOLE ANTENNA

In this Section, we will apply the proposed methodology to the analysis of an SWO connected to a monopole antenna.

First of all, the input impedance ($Z_A(f)$) of the monopole antenna with a finite radius over an infinite ground plane was calculated by solving the Hallen's integral equation using the method of moments [11]. Then, the transfer function $T(f)$ and the input voltage of the antenna, $V_A(f)$, were computed using equations (13) and (14), respectively. Figure 12 shows a plot of the imput impedance of the monopole, Z_A, as a function of frequency. Notice the resonance of the monopole at 201 MHz. The dimensions of the monopole are $L_m = 34.3$ cm, $r_m = 1.0$ cm.

The magnitude of the voltage transfer function $T(f)$ is shown in Figure 13. As it can be seen, $T(f)$ maximizes nearly at the resonance frequency and at the third harmonic.

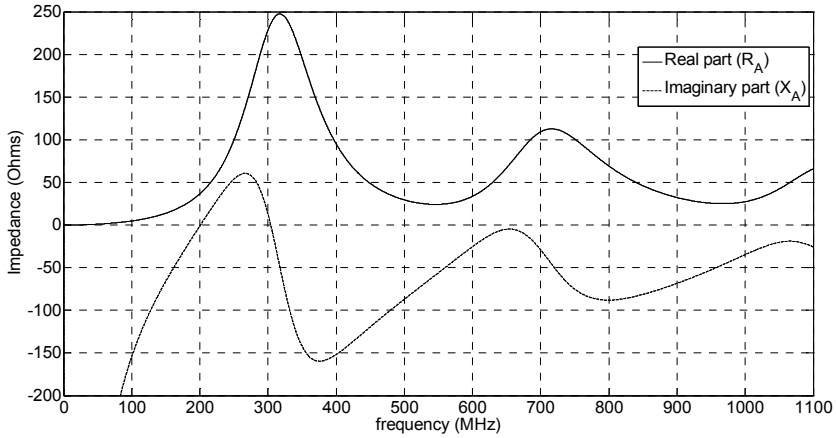

Figure 12 Input impedance of the monopole calculated using the method of moments. The dimensions of the monopole are $L_m = 34.9$ cm, $r_m = 1.0$ cm

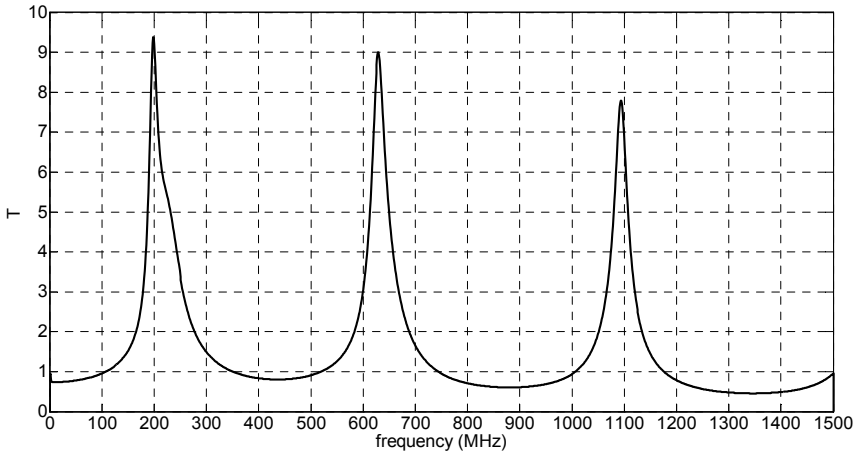

Figure 13 Voltage transfer function of the SWO connected to the monopole. Notice that the resonance frequency is slightly lower than the intended 200 MHz

Figure 14 presents the voltage at the input of the antenna in the frequency domain and in the time domain. This was calculated by using the input voltage $V_1(f)$ presented in Figure 7. As it can be seen, the signal is resonating at 200 MHz and there is a minor resonance at 630 MHz.

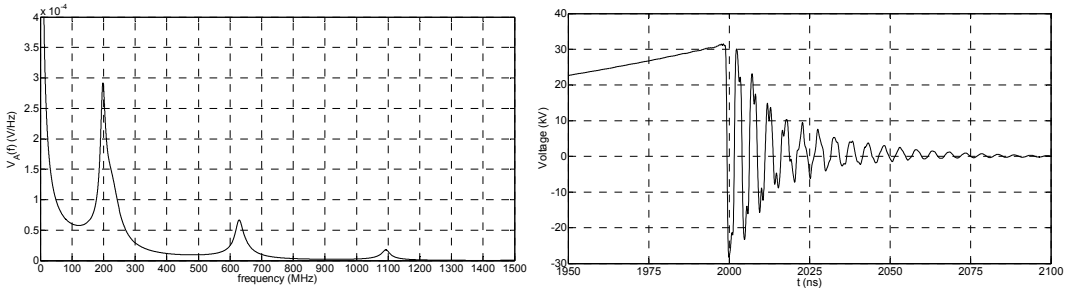

Figure 14 Voltage at the antenna in frequency (left) and time domain (right)

The radiated far field (in the (θ,ϕ) direction) was calculated by using a procedure analogous to the one presented in [2]. The transfer function of the antenna was calculated in the frequency domain as:

$$F_A(f,r,\theta,\phi) = \frac{E_\theta(f,r,\theta,\phi)}{V_A(f)} \tag{22}$$

This function gives the radiated electric field $(E_\theta\ (f,r,\theta,\phi))$ in the far range, at a given direction defined by angles (θ,ϕ), and distance (r), as a function of the applied voltage at the antenna terminals. The vertical electric field $E_\theta(f,r,\theta,\phi)$ was calculated by using the method of Moments [11]. A constant excitation $V_A(f)=1\ V$ was applied to the antenna and the electric field at a distance r=10 m and θ=90° was computed. Notice that since the antenna is

omnidirectional in the H-plane, there is no need to specify the azimuthal angle ϕ. A plot of the calculated transfer function is presented in Figure 15.

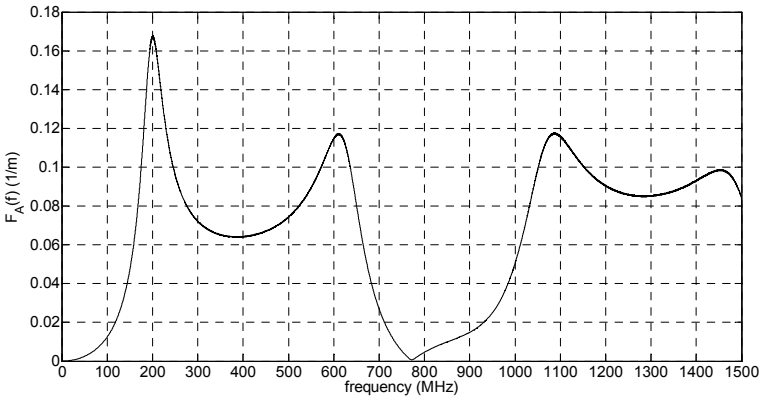

Figure 15 Transfer function of the antenna, at r=10 m, θ= 90°

Finally, the electric field radiated by the SWO (at the same coordinates) can be obtained by multiplying $F_A(f)$ and the voltage obtained with equation (13).

$$E_\theta(f,r,\theta,\phi) = V_A(f)F_A(f,r,\theta,\phi) = V_1(f)T(f)F_A(f,r,\theta,\phi) = \frac{Z_A(f)V_1(f)F_A(f,r,\theta,\phi)}{Z_A(f)A_{Total}(f)+B_{Total}(f)} \quad (23)$$

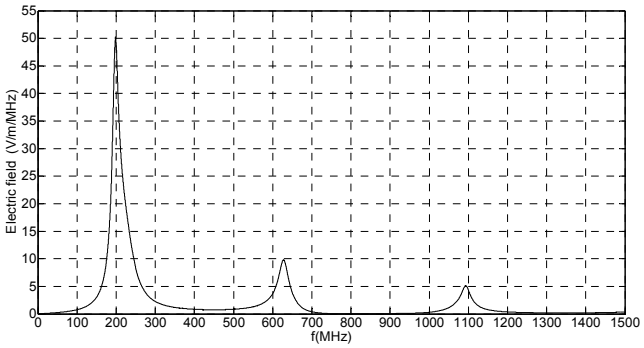

Figure 16 Radiated electric field in the frequency domain, corresponding to the input voltage presented in Figure 7

A plot of the radiated field in the frequency domain is presented in Figure 16, considering the excitation voltage given by Equation (15) and presented in Figure 7. As expected the resonance frequency is 200 MHz. The half amplitude bandwidth is BW=28 MHz, defined between f_L=188 MHz and f_H=216 MHz. The quality factor can be calculated as:

$$Q = \frac{f_0}{BW} = 7.1 \quad (24)$$

The expression derived in equation (23) can be rearranged in order to define a new transfer function relating the applied voltage and the radiated electric field ($T_{SWO}(f,\theta,\phi)$), independently of the observation distance (if the far field assumption is maintained):

$$T_{SWO}(f) = \frac{E_\theta(f,r,\theta,\phi)}{V_1(f)} r = \frac{Z_A(f) F_A(f,r,\theta,\phi)}{Z_A(f) A_{Total}(f) + B_{Total}(f)} r \tag{25}$$

This function can be used for optimization purposes. For example, if we want to maximize the field radiated at a certain frequency and direction, we can change the $F_A(f)$ and $Z_A(f)$ via either analytical modeling or simulation, up to reaching the desired response.

The resulting radiated field in time domain can be obtained by applying an inverse Fourier transform to the previously calculated electric field in the frequency domain. A plot of the radiated electric field in time domain is presented in Figure 17. The peak amplitudes of the wave are about +- 3.5 kV/m. Notice that, due to the symmetry of the antenna, the electric field is the same for all the points on the H-plane of the antenna at a the same distance *r*.

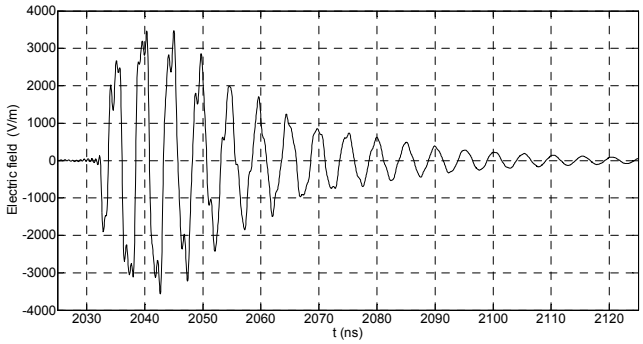

Figure 17 Radiated electric field in time domain in direction θ, at r=10 m, θ=90°

9. CONCLUSIONS

In this paper, we presented an analysis of a SWO using the chain-parameter (ABCD) representation of the system, which allows obtaining a semi-analytical solution suitable for the design and optimization of the SWO. In the analysis, all the constitutive parts of the SWO, namely the spark gap, the RTL, the coaxial TL, the blocking capacitor and the antenna were considered. Furthermore, the frequency dependence of the input impedance of the antenna was included in the analysis.

It was shown that by inspecting the frequency behavior of *A* and *B* parameters of the cascaded sections, the resonance frequencies and the output amplitudes can be predicted. This enables the possibility of "tailoring" the output by controlling the frequency behavior of each of the aforementioned sections.

The effect of connecting a spark gap at the input of the cascade was also assessed and it was shown that the output can be significantly modified depending on the value of the arc resistance. The effect of connecting a blocking capacitor was also observed.

Finally, the proposed method was used in the analysis of an SWO connected to a monopole antenna for which the transfer function and the radiated field were evaluated in the frequency domain and in the time domain.

Acknowledgments

This work is financially supported by the EPFL-SDC (Swiss Agency for Development and Cooperation) Fund.

10. REFERENCES

[1] C. E. Baum, "Switched Oscillators," *Circuit and Electromagnetic System Design Notes,* 200.

[2] D. V. Giri*, et al.*, "Switched Oscillators and Their Integration Into Helical Antennas," *Plasma Science, IEEE Transactions on,* vol. 38, pp. 1411-1426, 2010.

[3] M. Armanious*, et al.*, "Interaction Between Geometric Parameters and Output Waveforms in High-Power Quarter-Wave Oscillators," *Plasma Science, IEEE Transactions on,* vol. 38, pp. 1124-1131, 2010.

[4] F. Vega*, et al.*, "Design and optimization of mesoband radiators using chain parameters," in *Electromagnetics in Advanced Applications (ICEAA), 2011 International Conference on*, 2011, pp. 1310-1313.

[5] D. M. Pozar, *Microwave Engineering*, 3 ed.: Wiley, 2004.

[6] M. Abramowitz and I. Stegun, *Handbook of mathematical functions*: National Bureau of Standards, 1972.

[7] E. N. Protonotarios and O. Wing, "Analysis and Intrinsic Properties of the General Nonuniform Transmission Line," *Microwave Theory and Techniques, IEEE Transactions on,* vol. 15, pp. 142-150, 1967.

[8] T. Liu and F. Tesche, "Analysis of antennas and scatterers with nonlinear loads," *Antennas and Propagation, IEEE Transactions on,* vol. 24, pp. 131-139, 1976.

[9] T. H. Martin*, et al.*, *J.C. Martin on Pulsed Power*: Springer, 1996.

[10] D. V. Giri*, et al.*, "Intermediate and far fields of a reflector antenna energized by a hydrogen spark-gap switched pulser," *IEEE Transactions on Plasma Science,* pp. 1631-1636, 1999.

[11] C. A. Balanis, *Antenna Theory: Analysis and Design*, 3 ed., 2005.